Modelling drug release from polymer-free coronary stents with microporous surfaces

Tuoi T.N. Vo[a], Sarah Morgan[b], Christopher McCormick[b], Sean McGinty[c,*], Sean McKee[d], Martin Meere[e]

[a] MACSI, Department of Mathematics and Statistics, University of Limerick, Limerick, Ireland
[b] Department of Biomedical Engineering, University of Strathclyde, Glasgow G4 0NW, UK
[c] Division of Biomedical Engineering, University of Glasgow, Glasgow G12 8QQ, UK
[d] Department of Mathematics and Statistics, University of Strathclyde, Glasgow G1 1XH, UK
[e] Department of Applied Mathematics, NUI Galway, Galway, Ireland

ABSTRACT

Traditional coronary drug-eluting stents (DES) are made from metal and are coated with a permanent polymer film containing an anti-proliferative drug. Subsequent to stent deployment in a diseased coronary artery, the drug releases into the artery wall and helps prevent restenosis by inhibiting the proliferation of smooth muscle cells. Although this technology has proven to be remarkably successful, there are ongoing concerns that the presence of a polymer in the artery can lead to deleterious medical complications, such as late stent thrombosis. Polymer-free DES may help overcome such shortcomings. However, the absence of a rate-controlling polymer layer makes optimisation of the drug release profile a particular challenge. The use of microporous stent surfaces to modulate the drug release rate is an approach that has recently shown particularly promising clinical results. In this study, we develop a mathematical model to describe drug release from such stents. In particular, we develop a mathematical model to describe drug release from microporous surfaces. The model predicts a two-stage release profile, with a relatively rapid initial release of most of the drug, followed by a slower release of the remaining drug. In the model, the slow release phase is accounted for by an adsorption/desorption mechanism close to the stent surface. The theoretical predictions are compared with experimental release data obtained in our laboratory, and good agreement is found. The valuable insights provided by our model will serve as a useful guide for designing the enhanced polymer-free stents of the future.

1. Introduction

1.1. Background

Coronary Heart Disease (CHD) remains the leading cause of death globally, being responsible for around 16% of all deaths annually in high-income countries (WHO, 2014). Although medical treatments can be used to manage the symptoms in the early stages of the disease, more advanced cases ultimately require revascularisation of the affected vasculature to reduce the risk of myocardial infarction and heart failure. Despite the fact that coronary artery bypass graft revascularisation procedures are still commonly performed, with some evidence of better long-term outcomes for patients with multi-vessel disease and/or existing co-morbidities (Mohr et al., 2013; Park et al., 2015), the majority of coronary revascularisations are now performed by percutaneous coronary intervention (PCI).

In PCI, a balloon-mounted stent is expanded into the artery wall to restore blood flow through the affected lesion (Topol and Teirstein, 2015). Following withdrawal of the balloon, the stent provides permanent mechanical support to the vessel wall. Although the use of bare metal stents (BMS) represented a significant improvement on balloon angioplasty alone, BMS suffered from relatively high rates of in-stent restenosis (ISR) (Mehran et al., 1999) due, at least in part, to excessive smooth muscle cell (SMC) proliferation within the vascular wall (Marx et al., 2011). It was found that local release of anti-proliferative drugs from the stent surface could inhibit this proliferative response, with the first two drug-eluting stents (DES) (Pache et al., 2005; Stone et al., 2005) achieving quite dramatic reductions in ISR. However, these early generation devices were also associated with late-stent thrombosis (McFadden et al., 2004; Joner et al., 2006; Virmani et al., 2004). Although the precise causes of late-stent thrombosis remain to be determined, discontinuation of dual anti-platelet therapy has been associated with its occurrence, indicating incomplete restoration of a

functional endothelium (McFadden et al., 2004). Further evidence in support of this came from post-mortem and angiographic investigations that demonstrated that complete recovery of the endothelium was much more rapidly achieved in those patients who had been treated with a bare metal stent, compared to a first generation DES (Joner et al., 2006; Kotani et al., 2006). Such findings provided the stimulus for the development of alternative DES, making use of alternative drugs and coating technologies (Iqbal et al., 2013). There has since been a trend towards the use of analogues of rapamycin, with the latest devices increasingly using either biodegradable or polymer-free drug coatings to provide sustained release of the drug.

Stents featuring biodegradable polymer coatings (Abizaid and Costa, 2010; Guo et al., 2009) include the Biomatrix Stent (Biosensors International), the DESyne BD NOVOLIMUS Stent (Elixir Medical Corporation), the Nobori Stent (Terumo), the COMBO Dual Therapy Stent (OrbusNeich), and the Supralimus-Core Stent (SMT). In recent years, companies have also been pursuing the development of fully bioresorbable stents (Huang et al., 2014; Byrne and Kastrati, 2015), examples of these being provided by the Absorb Stent (Abbott Vascular) and the DESolve Stent (Elixir Medical Corporation).

Polymer-free stents abandon the use of a polymeric drug carrier altogether and instead employ technologies that are usually (though not always) based on directly covering a bare surface of the stent strut with drug (Khan et al., 2013; Chen et al., 2015). This surface may be relatively smooth, as in the case of the Amazonia Pax Stent (MINVASYS), or may be specially modified to receive the drug and modulate its subsequent release rate. In the latter case, microporous surface technology is the most commonly used in the manufacture of currently available polymer-free stents. A microporous surface contains pits whose breadth, depth and separation are on the order of micrometres in scale, and the Yukon (Translumina therapeutics, 2016), Yinyi (Yinyi Biotech, 2016), Vestasync (MIV Therapeutics) and Biofreedom (Biosensors International) stents are all examples of devices that employ this technology. Some nanoporous systems for drug delivery from stents have also been investigated (Kang et al., 2007; Tsujino et al., 2007).

The mathematical modelling of drug delivery in general (Siepmann and Siepmann, 2008; Peppas and Narasimhan, 2014), and drug delivery in the context of DES in particular (Tzafriri et al., 2012; O'Brien et al., 2013; McGinty, 2014), has received considerable attention in the literature in recent decades. Mathematical modelling provides a potentially powerful tool in the analysis and design of drug delivery systems. Such models can help optimise the design of a particular drug delivery system by guiding what device geometry, composition and drug-loading should be selected to achieve a desired release profile. This in turn can lead to a reduction in the number of experiments required for product development, with consequent savings in time and expense. More fundamentally, it is sometimes not even clear what the dominant drug delivery mechanisms in a particular system are, and mathematical modelling in conjunction with experimental data can assist in identifying these.

To our knowledge, there are no existing modelling studies that focus on drug release from microporous stent surfaces. However, there does exist some limited modelling studies on nanoporous surfaces that are of relevance. Gultepe et al. (2010) developed a model to describe drug release from a nanotubular metallic surface. Although they characterised their systems as being nanotubular, they did consider drug-filled tubes that had diameters as large as $0.2\,\mu m$. They assumed that the drug release was due to a desorption process in which the drug molecules have to overcome an activation energy barrier before leaving the surface. The activation energy was assumed to depend quadratically on the surface coverage of drug, and the resulting model produced results that matched their experimental data. In a more recent study, Tzur-Balter et al. (2013) developed a diffusion-based mathematical model to describe drug release from an eroding porous silicon surface. However, the pore diameters

considered in their study were significantly smaller than a micrometre. Finally, our group have recently reported on the development of mathematical models for nanoporous, nanotubular and smooth surface systems (McGinty et al., 2015). In the current study, we develop mathematical models to describe drug release from microporous surfaces. In McGinty et al. (2015), we consider drug diffusion through nanoporous and nanotubular systems, and these are *bulk* phenomena that require the consideration of material porosities. However, in the current study, we model drug release from a microporous surface, and the novel features of the behaviour here are *surface*-dominated. The emphasis here will be on DES, although our results may also be applicable more generally to any drug delivery device that employs microporous technology to modulate the drug release rate.

1.2. Outline

In this paper, we provide a model to describe the elution of drug from microporous DES. We start by describing the typical drug release experiment that we wish to model. We then formulate a system of one-dimensional coupled reaction-diffusion equations describing the drug release and demonstrate that these reduce to a single diffusion equation with a spatially varying diffusion coefficient, after making some reasonable assumptions. The release of drug is in two parts: a fast release phase for the bulk of the drug followed by a slow release phase for drug located close to the surface. Starting with the assumption of an unstirred release medium and no medium replacement at measurements, we are able to derive an analytical solution for the first phase of release. Subsequent release when the surface region has been exposed is solved for numerically. For the case of an unstirred release medium with medium replacement at each measurement, we derive an analytical solution for the release profile for both phases of the release. This solution is compared with our *in vitro* experimental data of drug release from the Yukon stent. The model is shown to capture the release profile well, and moreover we show how it is possible to inversely estimate unknown parameters in the system. *Remarkably we are able to demonstrate mathematically that if the switchover point between the initial fast release and slow release phases can be determined from the experimental release profile, then the first phase of the release is determined solely from the coordinates of this point.* Finally, we provide a mathematical model for the well-stirred case.

We stress that the models presented here are for drug release in an *in vitro* environment: such *in vitro* testing is an important part of early-stage DES design since it helps to give an indication of the release profiles that can be obtained from a prototype stent platform as well as verifying the repeatability of the drug release profiles.

2. Experimental methods

2.1. Characterisation of stent surface topography

Atomic force microscopy (AFM) (MFP 3D, Asylum Research, CA, USA) was used to characterise the surface features of three uncoated stainless steel Yukon Choice 4 (3 mm × 8 mm) stents. A small sample from each stent, consisting of a limited number of struts, was cut free from the expanded stent and adhered onto a glass slide. AFM scans were then performed in intermittent contact mode in air, imaging four random points on each stent surface. All scans were performed at a frequency of 1 Hz with scan sizes ranging from 1 to 20 μm. Representative images obtained are shown in Fig. 1 from which we observe that the depth, breadth and separation of the surface pits are of the order of micrometres in scale. Rapamycin coated Yukon stents, on the other hand, have previously been shown to be markedly smoother than their bare metal equivalents (Wessely et al., 2005).
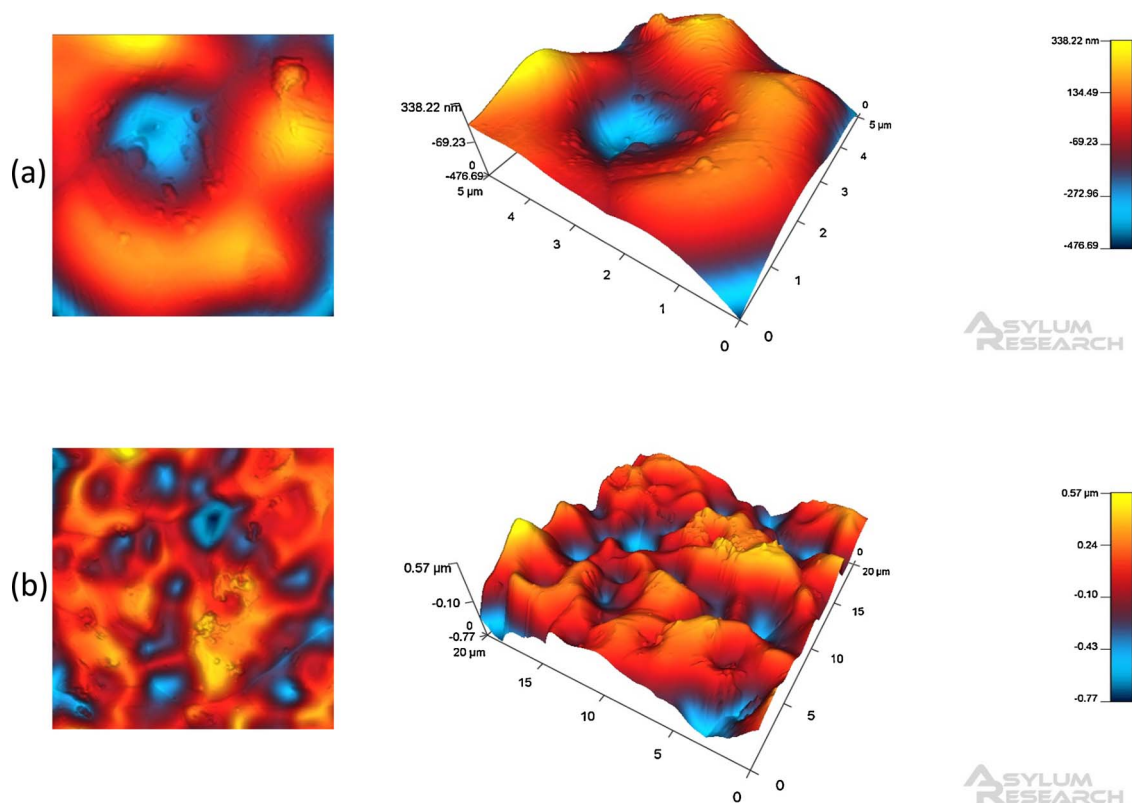
Fig. 1. Atomic force microscopy images of the surface of the Yukon Choice stent. Images are representative of three separate stent surfaces, each imaged at four randomly selected locations, at a scan size of (a) 5 μm and (b) 20 μm. Left hand panels are 2D orthographic projections with the corresponding 3D image shown on the right hand panels. The depth, breadth and separation of the surface pits are of the order of micrometres in scale.

2.2. In vitro drug release experiments

The surface of a Yukon Choice stent (3 mm × 16 mm) was coated once using a solution of rapamycin (10 mg/ml) in ethanol. The Translumina dose-adjustable coating machine was used to apply the coating according to the manufacturer's instructions. The drug coated stent was placed in a glass vial containing 2 ml of release medium (phosphate buffered saline:ethanol (90:10)). The stent was then removed to a separate glass vial containing fresh release medium at each of the following time points: 10 min, 1, 2, 6 h, 1, 3, 7, 14 and 28 days. The drug-containing release medium from each time point was stored at −20 °C prior to further analysis. All experiments were performed in unstirred release media maintained at 37 °C. The samples collected were analysed using UV-spectroscopy, with the peak absorbance measured at a wavelength of 279 nm being used to estimate the rapamycin release from the stent surface. At the end of the release experiment, the stent was transferred to a glass vial and stored at −20 °C. In order to determine if any rapamycin was left on the stent after the 28 day incubation period, it was brought to room temperature and then immersed in 2 ml of cold methanol overnight. The rapamycin in the methanol solution was then analysed by UV spectroscopy as previously described. There was no residual rapamycin detected in the methanol solution, indicating that complete release of the initial drug mass coated on to the stent (193 μg) had occurred within the 28 day release period.

## 3. The mathematical model

3.1. Preamble

In Fig. 2(a), we schematically depict a layer of drug covering a microporous surface. The surface contains pits whose depth, diameter and separation are of the order of micrometres in size. The system is placed in a release medium and the drug dissolves. Throughout this paper, we shall assume that the drug dissolves from its exposed surface only and that fluid does not penetrate the drug interior. For systems in which there is significant fluid ingress into the drug bulk, effects such as fragmentation may be significant and the analysis presented here may not then be appropriate. However, it should be noted that the classical dissolution models do not take account of fragmentation (Siepmann and Siepmann, 2013; Dokoumetzidis and Macheras, 2006; Costa and Lobo, 2001), although there are some studies that do incorporate the effect (Mangina et al., 2006).

A typical drug molecule has dimensions on the order of nanometres, and this is three orders of magnitude smaller than the typical dimensions of the microporous pits. Hence surface roughness on the scale of micrometres will not in general significantly affect the dissolution behaviour of individual drug molecules. However, surface roughness on submicron scales (see Fig. 2(a)) can have a significant effect – for example, on a lengthscale of nanometres, there may be van der Waals interactions between the drug molecules and the surface. A surface that is rough on a number of different length scales may have a relatively large surface area, so that a significant proportion of the drug loaded may be influenced by short-range surface effects. These effects will be incorporated into the modelling of the current study.

3.2. The unstirred case

Based on the images of the stent surface obtained (see Fig. 1), we consider a microporous surface as shown schematically in Fig. 2(a). The surface is covered with drug and placed in an unstirred release medium. In Fig. 2(a), we have indicated the location of the mean plane of surface roughness for the microporous surface. For the purposes of formulating a useable mathematical model, we replace the microporous surface by the mean plane. We suppose that the mean plane is located at $x = 0$ and that uniform solid drug now occupies the region above the plane. At first sight, this might seem a crude assumption. However, for the
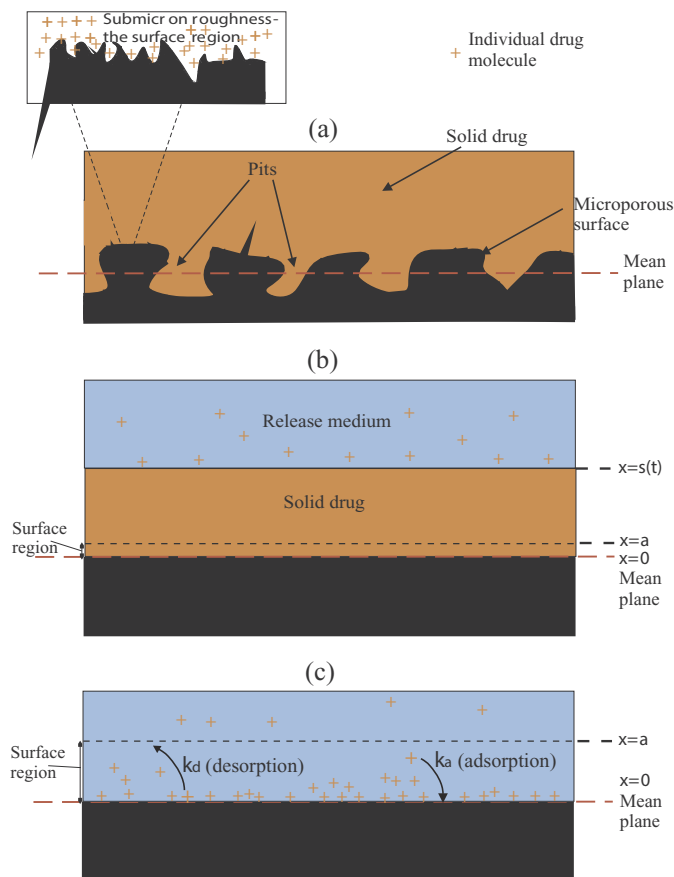
Fig. 2. (a) A microporous surface is covered with solid drug. The surface contains pits whose depth, diameter and separation are on the order of micrometres in size. The mean plane of the surface roughness is indicated on the figure. The blow-up shows that the surface is also rough on a submicron scale, and the surface region indicated refers to the narrow region close to the surface where the effects of adsorption and desorption can be significant. (b) To make the problem mathematically tractable, we replace the microporous rough surface by the mean plane. However, we do include a surface region in the modelling where adsorption to and desorption from the surface can be important effects. The system is placed in a release medium, and the solid drug begins to dissolve. A moving boundary $x = s(t)$ separates the undissolved drug from the release medium. In the system as depicted, the surface region is not yet exposed so that adsorption/desorption cannot occur. (c) At this stage of the release, the surface region is exposed, and adsorption/desorption become significant effects.

scenarios we are envisaging here, it does have justification since the dissolution of most of the drug in the microporous pits (see Fig. 2(a)) is unaffected by the surface; recall that the pits have dimensions on the order of micrometres, whereas the range of influence of the surface is on the order of nanometres. This aligns well with the observed biphasic release profile shown in Fig. 5(b).

When the system is placed in a release medium, it dissolves from its exposed surface, and a moving boundary $x = s(t)$ separates the un-dissolved drug from the release medium as shown in Fig. 2(b). The surface region is defined to be the neighbourhood of $x = 0$ where adsorption to and desorption from the surface are non-negligible effects, and we take this to occupy $0 < x < a$. Fig. 2(b) depicts the system at a stage when the drug still covers the surface region, so that surface effects do not enter. However, once the surface region has been exposed, adsorption/desorption become significant effects (Fig. 2(c)).

We shall develop a mathematical model that tracks the evolution of two distinct species of drug: free drug dissolved in the release medium and bound drug adhering to the rough surface. We denote by $b(x, t)$ and $c(x, t)$ the concentrations of bound drug and free drug, respectively, at location x and time t. The concentrations for b and c can only change in the region $x > s(t)$, and so we need only display equations for this

region. Since the release medium is taken to be unstirred here, diffusion is the only transport mechanism in the bulk of the fluid, and we have

$$\frac{\partial c}{\partial t} = D_w \frac{\partial^2 c}{\partial x^2} - k_a(x)c + k_d(x)b, \quad x > s(t), \quad t > 0, \tag{1}$$

$$\frac{\partial b}{\partial t} = k_a(x)c - k_d(x)b, \quad x > s(t), \quad t > 0, \tag{2}$$

where

$$k_a(x) = \begin{cases} k_a & \text{if } 0 < x < a, \\ 0 & \text{if } x > a, \end{cases} \quad k_d(x) = \begin{cases} k_d & \text{if } 0 < x < a, \\ 0 & \text{if } x > a, \end{cases} \tag{3}$$

and where D_w, k_a and k_d are constants. Here D_w is the diffusion coefficient for the free drug, and k_a and k_d are parameters characterising the rate of drug adsorption and desorption, respectively. The forms chosen for $k_a(x)$ and $k_d(x)$ in (3) ensure that drug adsorption and desorption are restricted to the surface region only. It should be emphasised here that $b(x, t) = 0$ for all $x > a$, $t > 0$.

It is noteworthy in (1) and (2) that we have not taken the adsorption rate $k_a(x)c$ to be dependent on the concentration of binding sites. This assumption is valid when the concentration of available binding sites greatly exceeds the concentration of adsorbate molecules so that the concentration of binding sites may be taken to be constant. However, models have previously been proposed that do track the concentration of binding sites; see, for example, the Langmuir model (Attard and Barnes, 1998) for the adsorption of gaseous molecules to a solid surface.

Adding (1) to (2) gives

$$\frac{\partial}{\partial t}(c + b) = D_w \frac{\partial^2 c}{\partial x^2}, \quad x > s(t), \quad t > 0, \tag{4}$$

an equation describing the evolution of the total drug concentration. For $x > s(t) > a$, we have $\partial b/\partial t = 0$, so that

$$\frac{\partial c}{\partial t} = D_w \frac{\partial^2 c}{\partial x^2}, \quad x > s(t) > a, \quad t > 0. \tag{5}$$

For $s(t) < x < a$, we have

$$\frac{\partial b}{\partial t} = k_a c - k_d b, \quad s(t) < x < a, \quad t > 0. \tag{6}$$

We assume here that the adsorption/desorption processes equilibrate on a time scale that is short compared to the other time scales arising in the system, so that (6) can be replaced by

$$b(x, t) = k_a c(x, t)/k_d, \quad s(t) < x < a, \quad t > 0. \tag{7}$$

Substituting (7) in (4) now gives

$$\frac{\partial c}{\partial t} = D_e \frac{\partial^2 c}{\partial x^2}, \quad s(t) < x < a, \quad t > 0, \tag{8}$$

where

$$D_e = \frac{D_w}{1 + 1/K_d} < D_w, \tag{9}$$

and where $K_d = k_d/k_a$. Combining (5) and (8) gives

$$\frac{\partial c}{\partial t} = \frac{\partial}{\partial x}\left(D(x)\frac{\partial c}{\partial x}\right), \quad x > s(t), \quad t > 0, \tag{10}$$

where

$$D(x) = \begin{cases} D_e(< D_w) & \text{if } 0 < x < a, \\ D_w & \text{if } x > a. \end{cases} \tag{11}$$

Eq. (10) is an appealing result since it implies that the effect of the rough surface on the drug release rate may be incorporated in a position-dependent drug diffusion coefficient. Away from the surface, diffusion is 'fast' with $D(x) = D_w$, but in the neighbourhood of the surface, diffusion is 'slow' with $D(x) = D_e < D_w$.

We now supplement (10) with boundary and initial conditions

appropriate to the case of an unstirred release medium. We denote by c_s the solubility of the free drug in the release medium. The solubility is the maximum possible concentration of dissolved drug in the release medium, and at the interface between the undissolved drug and the medium, we suppose that c is at solubility, so that

$$c = c_s \quad \text{on} \quad x = s(t), \quad t > 0. \tag{12}$$

Sufficiently far into the release medium, the concentration of drug falls to zero, so that

$$c \to 0 \quad \text{as} \quad x \to \infty, \quad t > 0. \tag{13}$$

Notice that we have taken the release medium to be infinite in extent here. This is a reasonable assumption if the release medium has a representative lengthscale on the order of centimetres, which is the case for the experiments conducted for the current study. We suppose that at $t = 0$, the drug layer occupies $0 < x < L_d$ and that the initial concentration of undissolved drug is c_0. We then have the following initial conditions:

$$s(t = 0) = L_d, \quad c(x, t = 0) = 0 \quad \text{for} \quad x > L_d,$$
$$c(x, t = 0) = c_0 \quad \text{for} \quad 0 < x < L_d. \tag{14}$$

To obtain a well-posed problem, we need another boundary condition to determine the motion of $x = s(t)$, the moving dissolution front. This will be derived by invoking conservation of drug. For $s(t) > a$, the total amount of drug in the system is given by

$$m(t) = A \left\{ \int_0^a (1 + k_a/k_d)c_0 \; dx + \int_a^{s(t)} c_0 \; dx + \int_{s(t)}^\infty c \; dx \right\},$$

where A is the cross-sectional area of the drug-covered plane. Imposing $dm(t)/dt = 0$ for $s(t) > a$ now gives

$$0 = \frac{dm(t)}{dt} = A \left\{ c_0 \frac{ds}{dt} - c_s \frac{ds}{dt} + \int_{s(t)}^\infty D_w \frac{\partial^2 c}{\partial x^2} dx \right\}$$
$$= A \left\{ (c_0 - c_s) \frac{ds}{dt} - \left(D_w \frac{\partial c}{\partial x} \right)_{x=s(t)} \right\}$$

so that

$$- D_w \frac{\partial c}{\partial x} = \frac{ds}{dt}(c_s - c_0) \quad \text{on} \quad x = s(t), \quad s(t) > a. \tag{15}$$

A similar calculation for $s(t) < a$ gives that

$$- D_e \frac{\partial c}{\partial x} = \frac{ds}{dt}(c_s - c_0) \quad \text{on} \quad x = s(t), \quad s(t) < a. \tag{16}$$

Combining (15) and (16) now yields

$$- D(x) \frac{\partial c}{\partial x} = \frac{ds}{dt}(c_s - c_0) \quad \text{on} \quad x = s(t), \quad t > 0. \tag{17}$$

Combining the equations formulated above now provides the following well-posed initial boundary value problem for the free drug c:

$$\frac{\partial c}{\partial t} = \frac{\partial}{\partial x}\left(D(x) \frac{\partial c}{\partial x} \right), \quad x > s(t), \quad t > 0,$$
$$c = c_s, \quad -D(x)\frac{\partial c}{\partial x} = \frac{ds}{dt}(c_s - c_0) \quad \text{on} \quad x = s(t), \quad t > 0,$$
$$\tag{18}$$
$$c \to 0 \quad \text{as} \quad x \to \infty, \quad t > 0,$$
$$s(t = 0) = L_d, \quad c(x, t = 0) = 0 \quad \text{for} \quad x > L_d.$$

We shall discuss solutions to this problem in Section 4.

3.3. A well-stirred release medium

The formulation for the well-stirred case is very different from that for the unstirred case. When the medium is well-stirred, a boundary layer of poorly stirred fluid forms close to the surface of the dissolving drug layer (Siepmann and Siepmann, 2013; Levich, 1962). This layer is
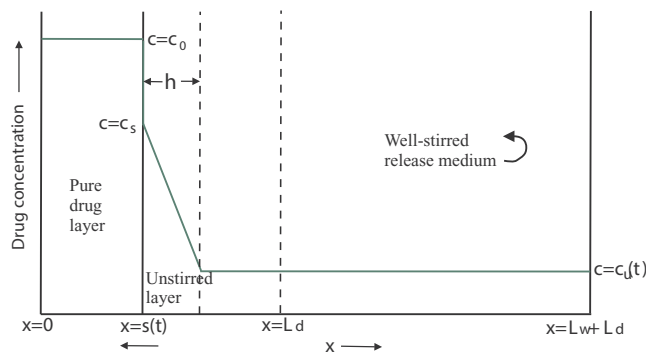

Fig. 3. In the case of a well-stirred release medium, a narrow boundary layer of poorly stirred fluid forms near the surface of the solid drug. The location of the pure drug surface is denoted by $x = s(t)$, and the system is depicted here at some time $t > 0$. It is assumed that the flux of drug from the dissolving surface is proportional to the difference between the drug concentration at the surface and the drug concentration in the well-stirred release medium. This schematic is not drawn to scale.

taken here to be of thickness h; the size of h depends on the degree of agitation in the fluid bulk. We shall take the release medium to be finite in extent and to initially occupy $L_d < x < L_w + L_d$ where L_d and L_w give the initial thicknesses of the drug and release medium, respectively. A moving boundary $x = s(t)$, initially located at $x = L_d$, separates the release medium from the pure drug layer. We assume here that $h \ll L_d \ll L_w$ and denote by $c_u(t)$ the spatially uniform drug concentration in the well-stirred medium at time t. In Fig. 3, we schematically depict the various regions and associated drug concentrations.

We assume here that the flux of drug from the surface of the dissolving drug layer is proportional to the difference between the concentration of drug in the release medium and the concentration of drug at the surface. Denoting by $j|_{x=s(t)}$ the flux of drug from $x = s(t)$, we write

$$j|_{x=s(t)} = -D(s(t)) \frac{(c_u(t) - c_s)}{h} \tag{19}$$

where c_s is the drug concentration on $x = s(t)$, and $D(s)$ is the position dependent diffusivity of the drug in the release medium as defined by (11). Eq. (19) can be regarded as a statement of Fick's first law of diffusion at $x = s(t)$. In view of (17), the appropriate equation for the speed of the front is now

$$- D(s) \frac{(c_u(t) - c_s)}{h} = \frac{ds}{dt}(c_s - c_0) \quad \text{for} \quad t > 0. \tag{20}$$

Equating the amount of drug that has dissolved with the amount in the release medium and using the assumptions that $h \ll L_d \ll L_w$ and $c_u(t) \ll c_0$, we have

$$(L_d - s(t))c_0 \approx L_w c_u(t). \tag{21}$$

Combining (20) and (21) leads to the following initial value problem for $s(t)$:

$$\frac{ds}{dt} + \frac{D(s)}{hL_w} \frac{c_0}{c_0 - c_s} s \approx \frac{D(s)}{hL_w} \frac{L_d c_0 - L_w c_s}{c_0 - c_s}, \quad t > 0, \tag{22}$$

$$s = L_d \quad \text{at} \quad t = 0.$$

We shall discuss the solution to this problem in Section 4.

3.4. Release profiles

We begin by considering the unstirred case. For the purposes of the current study, we define the total amount of drug *released* by the system at any time t to be the total amount of drug in solution in the release medium at this time. Denoting this quantity by $M(t)$, we have that

$$M(t) = A \int_{s(t)}^\infty c(x, t) dx,$$

where, recall, A is the cross-sectional area of the drug-covered plane. If we assume that $s(t) > a$, then

$$
\begin{aligned}
\frac{dM(t)}{dt} &= A\left(\int_{s(t)}^{\infty} \frac{\partial c}{\partial t} dx - \frac{ds(t)}{dt} c(s(t)^+, t)\right) \\
&= A\left(\left[D_w \frac{\partial c}{\partial x}\right]_{x=s(t)^+}^{\infty} - \frac{ds(t)}{dt} c_s\right),
\end{aligned}
$$

and if we now employ the second boundary condition in the second line of the equation list (18), we arrive at

$$
\frac{dM(t)}{dt} = -Ac_0 \frac{ds(t)}{dt}.
\tag{23}
$$

A similar calculation shows that (23) also holds for $0 < s(t) < a$. Integrating (23) subject to $M(0) = 0$, $s(0) = L_d$ gives

$$
M(t) = Ac_0(L_d - s(t)).
$$

All of the drug has dissolved by time $t = t_d$ where t_d is determined from $s(t_d) = 0$, and at this time, $M(t_d) = Ac_0 L_d$. Assuming that the boundary $x = 0$ is impermeable to drug, it is easily shown that $dM(t)/dt = 0$ for $t > t_d$, so that $M(t_d) = M(\infty) = Ac_0 L_d$. A release profile is a plot of the fraction of the total drug that has released as a function of time t, and it is given here by

$$
\frac{M(t)}{M(\infty)} = \begin{cases} 1 - s(t)/L_d & \text{for} \quad 0 \le t < t_d, \\ 1 & \text{for} \quad t \ge t_d. \end{cases}
\tag{24}
$$

A similar analysis shows that the formula for the release profile for the well-stirred case is also given by (24).

4. Results and discussion

4.1. The unstirred problem

We now consider the solution to the problem (18). For $s(t) > a$, the problem can be solved explicitly, and the details of the solution method can be found in McGinty et al. (2015). For $s(t) > a$, the solution is given by

$$
s(t) = L_d - \theta\sqrt{t}, \quad c = c_s \frac{\operatorname{erfc}\left(\frac{x - L_d}{2\sqrt{D_w t}}\right)}{\operatorname{erfc}\left(-\frac{\theta}{2\sqrt{D_w}}\right)}, \quad L_d - \theta\sqrt{t} < x < \infty,
\tag{25}
$$

where θ is determined by solving the nonlinear equation

$$
\frac{\theta}{2\sqrt{D_w}} \exp\left(\frac{\theta^2}{4D_w}\right) \operatorname{erfc}\left(-\frac{\theta}{2\sqrt{D_w}}\right) = \frac{1}{\sqrt{\pi}} \frac{c_s}{c_0 - c_s}.
\tag{26}
$$

This solution remains valid until $t = t_a$ where $s(t_a) = a$, so that

$$
t_a = \frac{(L_d - a)^2}{\theta^2}.
$$

For $t > t_a$, the governing equations are:

$$
\begin{aligned}
&\frac{\partial c}{\partial t} = \frac{\partial}{\partial x}\left(D(x)\frac{\partial c}{\partial x}\right), \quad x > s(t), \quad t > t_a, \\
&c = c_s, \quad -D_e \frac{\partial c}{\partial x} = \frac{ds}{dt}(c_s - c_0) \quad \text{on } x = s(t), \quad t > t_a, \\
&c \to 0 \quad \text{as} \quad x \to \infty, \quad t > t_a, \\
&s(t = t_a) = a, \quad c(x, t = t_a) = c_s \frac{\operatorname{erfc}\left(\frac{x - L_d}{2\sqrt{D_w t_a}}\right)}{\operatorname{erfc}\left(-\frac{\theta}{2\sqrt{D_w}}\right)} \quad \text{for} \quad x > a,
\end{aligned}
\tag{27}
$$

where θ is determined from (26). This problem cannot be solved analytically, and so we employed a front-tracking numerical scheme to

obtain approximate solutions. The details of the scheme can be found in Appendix A. The transition between the rapid and the slow release can be identified on the release profile shown in Fig. 5(a) and occurs at the point

$$
(t_a, M(t_a)/M(\infty)) = ((L_d - a)^2/\theta^2, 1 - a/L_d).
\tag{28}
$$

Eq. (28) is of value when assessing experimental data. If in an experimental release profile the transition point is clearly identifiable, then comparing the experimental result with the theoretical prediction (28) should enable the estimation of the parameters a and θ if L_d is known. Explicitly, a may be estimated using the formula

$$
a = L_d\left(1 - \frac{M(t_a)}{M(\infty)}\right)
\tag{29}
$$

and then

$$
\theta = \frac{L_d - a}{\sqrt{t_a}}.
\tag{30}
$$

Eq. (26) can now be used to provide an estimate for the free drug diffusion coefficient D_w if c_s/c_0 is known. Conversely, if D_w is known, (26) provides an estimate for c_s/c_0, which in turn can provide an estimate for the drug solubility c_s if c_0 is known.

Remarkably, it transpires that the first phase of the release profile is determined solely from the coordinates of this transition point. To see this, we combine (24) and (25) to obtain

$$
\frac{M(t)}{M(\infty)} = 1 - \frac{s(t)}{L_d} = \frac{\theta\sqrt{t}}{L_d} \quad \text{for} \quad 0 \le t < t_a,
$$

from which we deduce that

$$
\frac{M(t)}{M(\infty)} = \frac{M(t_a)}{M(\infty)}\sqrt{\frac{t}{t_a}} \quad \text{for} \quad 0 \le t < t_a.
\tag{31}
$$

The significance of this last result is that, if we can identify the transition point on the experimental release profile, then this is all the information we need to simulate the first phase of the release.
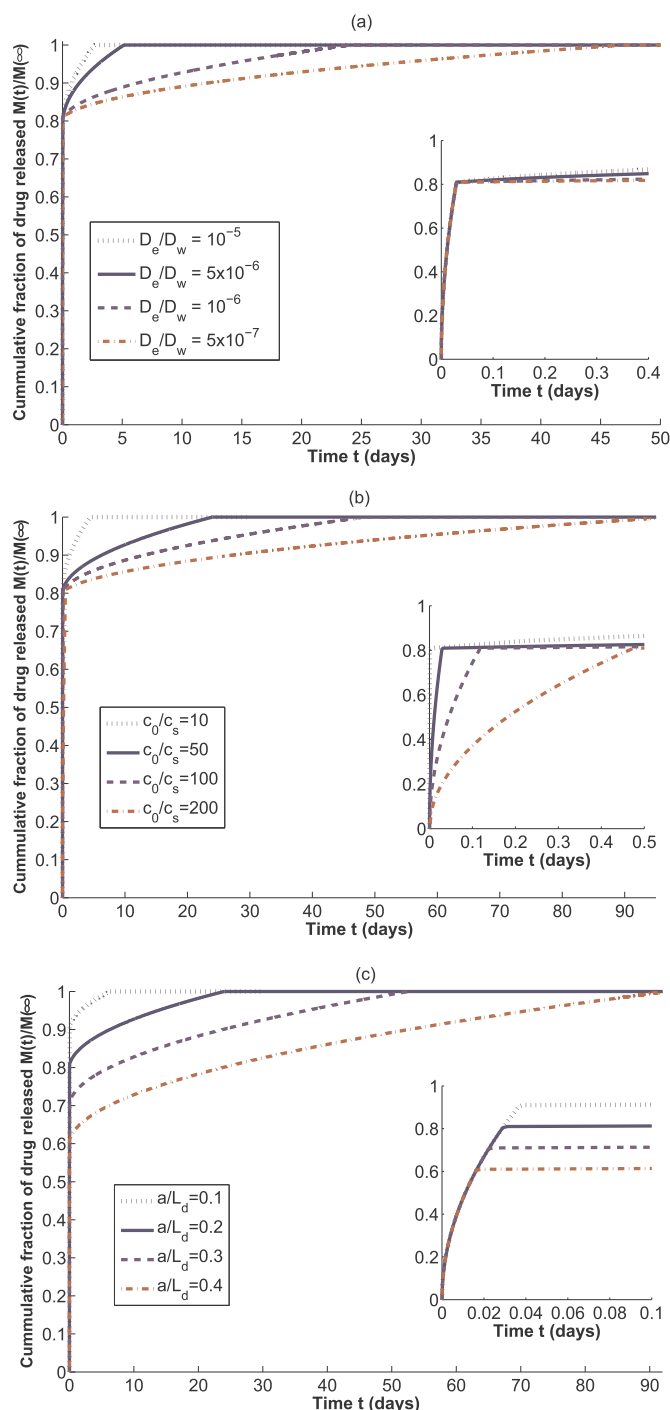
4.1.1. Numerical solutions

In Fig. 4, we display theoretically generated drug release profiles for the unstirred case where the release medium is not replaced. The curves were calculated using the formulae (24) and (25) and by numerically integrating (27) . The results illustrate the quite wide variety of release behaviours the system is capable of exhibiting. Fig. 4(a) shows the effect of varying the effective drug diffusion coefficient D_e in the surface region, and the results are as expected with the release rate in the slow phase decreasing with decreasing D_e. The effective diffusion coefficient depends on the adsorption/desorption properties of the drug molecules with the surface.

The effect of varying the drug solubility c_s is shown in Fig. 4(b). The behaviour here is seen to be strongly dependent on the solubility in the early rapid stage of the release (see the inset), with the curves exhibiting a quite dramatic slowing in the drug release rate with decreasing c_s. This behaviour can be understood by noting that for $c_s/c_0 \ll 1$, we have from (26) that $\theta \approx 2\sqrt{D_w/\pi}\, c_s/c_0$, so that

$$
t_a \approx (L_d - a)^2 \frac{\pi}{4D_w}\left(\frac{c_0}{c_s}\right)^2,
$$

implying that the duration of the rapid release phase depends on the square of the inverse of the drug solubility. This remark is consistent with the behaviour exhibited in the inset of Fig. 4(b).

In Fig. 4(c), we display release curves for various thicknesses of the surface region. For these curves, the initial stages of the profiles are identical because the surface plays no role in the release behaviour here. In designing a real system, changing a would correspond to

Fig. 4. Theoretically generated drug release profiles for the unstirred case without medium replacement. The curves were calculated using (24) and (25) and by numerically integrating (27). Here D_w is the diffusion coefficient of the drug in the release medium, D_e is the effective diffusion coefficient of the drug in the surface region, L_d is the initial thickness of the drug layer, a is the thickness of the surface region, c_0 is the initial concentration of the undissolved dry drug, and c_s is the solubility of the drug in the release medium. Unless stated otherwise on the figure, the parameter values used are $D_w = 5 \times 10^{-7}$ cm^2 s^{-1}, $D_e/D_w = 10^{-6}$, $L_d = 10$ μm, $a/L_d = 0.2$, and $c_0/c_s = 50$. In the plots, we display drug release profiles for (a) varying values of the effective drug diffusion coefficient in the surface region, (b) varying values of the solubility, and (c) varying thicknesses of the surface region.

changing the roughness characteristics of the surface. However, it should be stated that in the current study, no explicit connection has been made between the parameters appearing in the mathematical model and surface roughness parameters (Whitehouse, 2002).

Nevertheless, we can conclude that from the point of view of delaying the release of a larger fraction of the drug, roughness on both micron and submicron scales is preferable to roughness on submicron scales alone since the total surface area in the former case is larger. Larger surface areas imply that a larger fraction of the drug load is initially adhering to the surface, and this fraction releases more slowly. In terms of our modelling, larger surface areas correspond to larger values of the effective surface thickness parameter a.

4.1.2. Implications for choice of drug to be coated on microporous stents

Whilst biphasic kinetics are clearly a feature of these microporous stents, it is evident from Fig. 4 that the majority of the drug is released rapidly. Indeed, for the wide range of parameters that we have simulated, most of the drug is released within the first day. In order to evaluate the potential clinical significance of this finding, we must assess these rapid release profiles in the context of restenosis development, a process that occurs over a period of weeks after stent implantation.

We note that the drugs coated on early DES included heparin, paclitaxel and rapamycin. Early mathematical modelling (for example Hwang et al., 2001) helped explain the failure of hydrophilic heparin stents and the relative success of paclitaxel and rapamycin eluting stents, based on analysis of their partitioning and transport properties in arterial tissue. In particular, rapamycin and paclitaxel are extremely poorly soluble hydrophobic compounds that bind tenaciously to the arterial wall. Rapamycin is an anti-proliferative compound that targets the FK-binding protein 12 (FKBP12) (Daemen and Serruys, 2007). This complex subsequently binds to the mammalian target of rapamycin (mTOR) and thereby interrupts the cell cycle in the G1-S phase. Paclitaxel is also an anti-proliferative compound; however, it inhibits neointimal growth by binding with and stabilising microtubules, resulting in cell-cycle arrest in the G0–G1 and G2-M phases (Martin and Boyle, 2011).

Recently, mathematical modelling has been used to help explain how differences in the binding properties of rapamycin and paclitaxel lead to different drug persistence times in the wall, suggesting that the optimal delivery strategy is drug dependent (Bozsak et al., 2014). For example, whilst the timescale for binding of rapamycin (∼5 min) is much quicker than for paclitaxel (∼5 h), the timescale for unbinding of rapamycin (∼11 h) is considerably shorter than that of paclitaxel (∼210 h). Based on time scale analysis, Bozsak et al. (2014) postulated that paclitaxel-eluting stents perform optimally by releasing their drug either very rapidly (within a few hours) or very slowly (over periods of several months) (Bozsak et al., 2014), and in contrast, rapamycin-eluting stents perform optimally only when drug release is slow (Bozsak et al., 2014). The implication is that for the Yukon Choice stent studied here, coating with paclitaxel or a drug with similar binding properties may actually be preferable in terms of combating restenosis. Alternatively, strategies to slow the rapamycin release may be advantageous, and we note that the manufacturer of the stent under study is actively pursuing such approaches. Since the current state-of-the-art indicates that receptor saturation is strongly linked with efficacy (Tzafriri et al., 2012), we further note that it may, in principle, be possible to design a microporous stent where the rate of the second phase of release is tuned to match declining receptor saturation levels, thereby acting to replenish the drug in the tissue and prolonging receptor saturation.

4.1.3. Unstirred, replaced release medium

The situation we have described above assumes that the release medium is not changed between measurements. However, it is also common for the stent to be removed and placed in a fresh release medium between measurements. This strategy is typically adopted where there are constraints on the limit of detection of the drug. It is therefore of interest also to consider the case where the release medium is replaced. Mathematically this is modelled by a resetting of the drug

concentration to zero in the release medium at every measurement time point. Assuming that the transition time t_a between the fast release phase and the slow release phase corresponds to one of the measurement time points, the release profile can be computed using the following expression (see Appendix A for details):

$$\frac{M(t)}{M(\infty)} = \begin{cases} \dfrac{\theta\sqrt{t}}{L_d} & \text{for} \quad 0 \leq t < t_1, \\[2mm] \dfrac{\theta}{L_d}(\sqrt{t_1} + \sqrt{t - t_1}) & \text{for} \quad t_1 \leq t < t_2, \\ \vdots \\ \dfrac{\theta}{L_d}(\sqrt{t_1} + \sqrt{t_2 - t_1} + \cdots + \sqrt{t - t_{n-1}}) & \text{for} \quad t_{n-1} \leq t < t_n, \\[2mm] 1 - \dfrac{a}{L_d} + \dfrac{\theta^*}{L_d}\sqrt{t - t_n} & \text{for} \quad t_n \leq t < t_d, \\[2mm] 1 & \text{for} \quad t \geq t_d, \end{cases}$$

$$(32)$$

where t_i, $i = 1, \ldots, n - 1$ are the experimental time points before the transition, $t_n = t_a$ is the time of the transition and $t_d = t_n + a^2/\theta^{*2}$ is the time by which all of the drug has dissolved. In (32), θ and θ^* are both constant parameters, where θ is determined by solving (26) and θ^* is determined by solving (see Appendix A)

$$\frac{\theta^*}{2\sqrt{D_w}}\exp\left(\frac{\theta^{*2}}{4D_e}\right)\left(1 - \sqrt{\frac{D_w}{D_e}}\,\text{erf}\left(-\frac{\theta^*}{2\sqrt{D_e}}\right)\right) = \frac{1}{\sqrt{\pi}}\frac{c_s}{c_0 - c_s}. \qquad (33)$$

Once again, provided that L_d is known, a and θ can be estimated from the experimental data point $(t_a, M(t_a)/M(\infty))$. We can again estimate a using (29), and then

$$\theta = \frac{L_d - a}{\sqrt{t_1} + \sqrt{t_2 - t_1} + \cdots + \sqrt{t_n - t_{n-1}}}. \qquad (34)$$

We can now estimate D_w using (26) if c_s/c_0 is known or vice-versa.

4.1.4. Comparison with experimental data

In Fig. 5, we display the results of the release experiment described in Section 2.2. Fig. 5(b) shows the measured drug release profile plotted against the square root of time. The release profile is clearly biphasic, i.e. there is a clear transition point separating a fast initial rate of release from a subsequent slower rate of release. A simple single phase dissolution model (McGinty et al., 2015) is incapable of replicating such behaviour.

In Fig. 5(a), we compare the theoretical profile (32) with the experimentally measured release profile plotted as a function of time. In order to use the formula (32), values for the parameters θ/L_d, a/L_d, θ^*/L_d and $t_n = t_a$ must be selected that are consistent with (34), and values were chosen here to obtain a good fit with the experimental data. The values selected can be found in the caption of Fig. 5. It is noteworthy that it is not necessary to

explicitly choose values for D_w, k_a, k_d, c_0 and c_s to implement the fitting. However, these values will satisfy the constraints (26) and (33) and so may be deducible indirectly depending on which parameters are known for a particular system. The reverse question is also worth considering – what system parameters need to be known in advance in order to apply the model directly to a particular system without fitting? Inspecting Eqs. (26), (32), (33) and (34), it is seen that it is sufficient to specify values for D_w, D_e, c_s/c_0, L_d and a to implement the model.

The biphasic character of the release in Fig. 5(a) is clear, with a relatively rapid initial release of most of the drug, followed by a slower release of the remaining drug. The theory developed in this paper posits that the fast release here corresponds to dissolution of drug away from the surface region, while the slow release corresponds to drug dissolution in the surface region. It is clear that our mathematical model is capturing the experimentally observed release profile well.

4.2. The well-stirred problem

To obtain the solution for the well-stirred case, we must solve the initial-value problem (22). The solution to (22) for $s(t) > a$ is given by

$$s(t) = L_d - \frac{c_s}{c_0}L_w\left(1 - \exp\left(-\frac{D_w}{hL_w}\frac{c_0}{(c_0 - c_s)}t\right)\right). \qquad (35)$$

This solution remains valid until $t = t_a$ where $s(t_a) = a$. Using (35), we find that

$$t_a = -\frac{hL_w}{D_w}\frac{(c_0 - c_s)}{c_0}\ln\left(1 - \frac{c_0}{c_s}\frac{(L_d - a)}{L_w}\right). \qquad (36)$$

We remark that this quantity is only defined for $1 - c_0(L_d - a)/c_sL_w > 0$, or $c_sL_w > c_0(L_d - a)$. This corresponds to our intuitive expectations here since if $c_sL_w < c_0(L_d - a)$, the release medium would become fully saturated with drug before $s(t)$ could reach a, and dissolution would then cease.

For $t > t_a$, the motion of the moving boundary is governed by

$$\frac{ds}{dt} + \frac{D_e}{hL_w}\frac{c_0}{c_0 - c_s}s = \frac{D_e}{hL_w}\frac{L_dc_0 - L_wc_s}{c_0 - c_s}, \quad t > t_a, \qquad (37)$$

$$s = a \text{ at } t = t_a$$

and this has the solution

$$s(t) = \left(L_d - \frac{c_s}{c_0}L_w\right) - \left(L_d - \frac{c_s}{c_0}L_w - a\right)\exp\left(-\frac{D_e}{hL_w}\frac{c_0}{(c_0 - c_s)}(t - t_a)\right) \qquad (38)$$

for $t > t_a$. The time for all of the drug to dissolve, $t = t_d$, is determined by solving $s(t_d) = 0$. Using (38), this gives
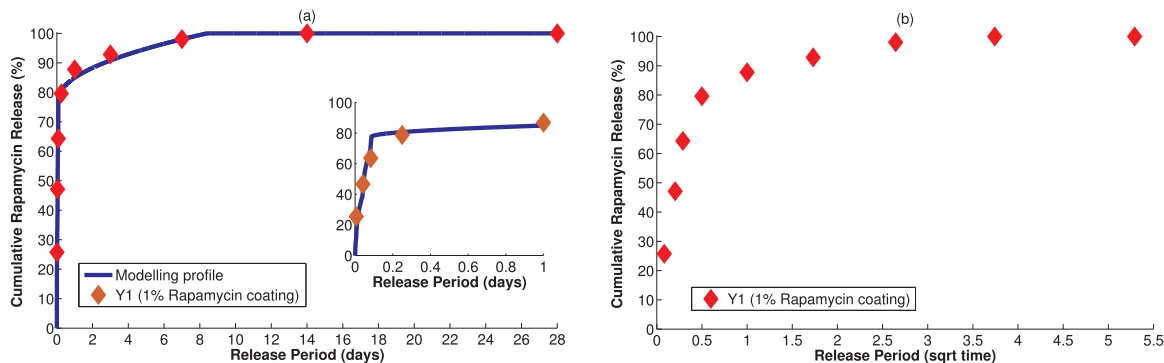

Fig. 5. (a) Comparison between experimental drug release data and the theoretical drug release profile (32). The solid curve shown is theoretical, and the parameter values used to generate it are $a/L_d = 0.225$, $\theta/L_d = 1.475$, $\theta^*/L_d = 0.078$ and $t_a = 0.086$ days. The diamonds give the experimental release data, and the inset highlights the release behaviour over the first day of release. (b) Plot of the experimental release data versus the square root of time.

$$t_d = t_a + \frac{hL_w}{D_e} \frac{(c_0 - c_s)}{c_0} \ln\left(1 + \frac{a}{c_s L_w / c_0 - L_d}\right).$$

Clearly for this to be physically meaningful we require that $t_d > t_a$, which implies that $c_s L_w / c_0 - L_d > 0$ or $c_s L_w > c_0 L_d$. This last condition implies that in order for t_d to be defined, the release medium must be capable of accommodating all of the drug before saturating. Finally for $t > t_d$, we clearly have $s(t) = 0$.

Combining the results above and using (24), we now have that

$$\frac{M(t)}{M(\infty)} = \begin{cases} \dfrac{c_s L_w}{c_0 L_d}\left(1 - \exp\left(-\dfrac{D_w}{hL_w}\dfrac{c_0}{(c_0 - c_s)}t\right)\right) & \text{for} \quad 0 \leq t < t_a, \\[2ex] \dfrac{c_s L_w}{c_0 L_d} + \left(1 - \dfrac{c_s L_w}{c_0 L_d} - \dfrac{a}{L_d}\right)\exp\left(-\dfrac{D_e}{hL_w}\dfrac{c_0}{(c_0 - c_s)}(t - t_a)\right) & \text{for} \quad t_a \leq t < t_d, \\[2ex] 1 & \text{for} \quad t \geq t_d. \end{cases} \tag{39}$$

5. Conclusions

Microporous drug release systems have surfaces that are rough on the micron scale; that is, the breadth, depth and separation of the surface pits have dimensions of the order of microns. However, the molecular dimensions of drug molecules are typically of the order of nanometres, three orders of magnitude smaller than the dimensions of the pits. Hence, for solid drug that dissolves from its surface interface with the release medium only, the dissolution behaviour of most of the drug molecules in the pits may not be significantly affected by the presence of the surface. Hence, the concept that roughness on the scale of the micron can in and of itself significantly retard the release of a substantial fraction of the drug may not be valid for some systems. However, roughness on submicron scales can significantly retard drug release via surface effects such as Van der Waals interactions; these forces act over a much shorter range than a micron. Nevertheless, such forces can still affect a significant amount of drug for systems whose surfaces are rough on both the micron *and* submicron scales since the total surface area can then be large. These observations motivated the development of the biphasic mathematical model presented in the current study.

The mathematical model developed here is, to the best of our knowledge, the first that attempts to model drug release from microporous surfaces. Although our model does incorporate a number of significant simplifying assumptions to enable analytical progress, it does successfully capture the key features of the experimentally observed release behaviour. We conducted drug release experiments for a Yukon stent coated with rapamycin and found that the release profile had a distinct two-stage character, with most of the drug releasing relatively rapidly over a period of about half a day, and the remainder of the drug releasing more slowly over a period of about a week. This biphasic character of the experimental release is captured very well by our theoretical model. In our theoretical formulation, the slow release phase is accounted for by an effective diffusion coefficient for the drug in the neighbourhood of the surface that is smaller than the free drug diffusion coefficient.

Simulations of the mathematical model indicate that microporous systems are capable of exhibiting quite a broad range of release behaviours. Amongst the parameters that may be used to tune the character of release profiles are the thickness of the drug layer and, of course, the surface roughness. Moreover, and more interestingly, we note that experimental release data in conjunction with theoretical profiles can be used to estimate key system parameters, such as the free drug diffusion coefficient.

Finally, we believe that it is appropriate to acknowledge that a number of assumptions have been made in this analysis. Firstly, we

replace the actual microporous surface by a mean plane representation, with our justification being that the dissolution of most of the drug in the microporous pits is unaffected by the surface. Secondly, we have assumed that the drug dissolves from its exposed surface only. Thirdly, we have not taken the drug absorption rate on the stent surface to be dependent on the concentration of binding sites, an assumption which is valid when the concentration of available binding sites greatly exceeds the concentration of absorbate molecules. In deriving our analytical solutions, we have assumed that the release medium is in-

finite in extent, which is a reasonable assumption when the length scale of the release medium is much greater than the diffusion length. Finally, the mathematical model presented does not account for the possibility of drug degradation in the release medium. A model which accounts simultaneously for drug release and degradation of drug is beyond the scope of this study and calls for the development of more sophisticated modelling approaches, which we will pursue in future work.

Research Data

All experimental data created during this research are openly available from the University of Strathclyde at https://doi.org/10.15129/b62281dc-08cf-4138-b6cc-db32beb200ab. The mathematical models and their solutions are detailed in the text and in the supplementary material.

Appendix A. Supplementary data

Supplementary data associated with this article can be found, in the online version, at https://doi.org/10.1016/j.ijpharm.2017.12.007.

References

Abizaid, A., Costa, J.R., 2010. New drug-eluting stents: an overview on biodegradable and polymer-free next-generation stent systems. Circ. Cardiovasc. Interv. 3, 384–393.

Attard, G., Barnes, C., 1998. Surfaces, first ed. Oxford University Press, Oxford.

Bozsak, F., Chomaz, J.M., Barakat, A.I., 2014. Modeling the transport of drugs eluted from stents: physical phenomena driving drug distribution in the arterial wall. Biomech. Model. Mechanobiol. 13 (2), 327–347.

Byrne, R.A., Kastrati, A., 2015. Bioresorbable drug-eluting stents: an immature technology in need of mature application. JACC Cardiovasc. Interv. 8 (1), 198–200.

Chen, W., Habraken, T.C.J., Hennink, W.E., Kok, R.J., 2015. Polymer-free drug-eluting stents: an overview of coating strategies and comparison with polymer-coated drug-eluting stents. Bioconjugate Chem. 26, 1277–1288.

Costa, P., Lobo, J.M.S., 2001. Modeling and comparison of dissolution profiles. Eur. J. Pharm. Sci. 13, 123–133.

Daemen, J., Serruys, P.W., 2007. Drug-eluting stent update 2007. Part I: A survey of current and future generation drug-eluting stents: meaningful advances or more of the same? Circulation 116 (3), 316–328.

Dokoumetzidis, A., Macheras, P., 2006. A century of dissolution research: from Noyes and Whitney to the biopharmaceutics classification system. Int. J. Pharm. 321, 1–11.

Gultepe, E., Nagesha, D., Casse, B.D.F., Banyal, R., Fitchorov, T., Karma, A., Amiji, M., Sridhar, S., 2010. Sustained drug release from non-eroding nanoporous templates. Small 6 (2), 213–216.

Guo, Q., Knight, P.T., Mather, P.T., 2009. Tailored drug release from biodegradable stent coatings based on hybrid polyurethanes. J. Controlled Release 137, 224–233.

Huang, Y., Ng, H.C.A., Ng, X.W., Subbu, V., 2014. Drug-eluting biostable and erodible stents. J. Controlled Release 193, 188–201.

Hwang, C.W., Wu, D., Edelman, E.R., 2001. Physiological transport forces govern drug distribution for stent-based delivery. Circulation 104 (5), 600–605.

Iqbal, J., Gunn, J., Serruys, P.W., 2013. Coronary stents: historical development, current status and future directions. Br. Med. Bull. 106, 193–211.

Joner, M., Finn, A.V., Farb, A., Mont, E.K., Kolodgie, F.D., Ladich, E., Kutys, R., Skorija, K., Gold, H.K., Virmani, R., 2006. Pathology of drug-eluting stents in humans: delayed healing and late thrombotic risk. J. Am. Coll. Cardiol. 48 (1), 193–202.

Kang, H., Kim, D.J., Park, S., Yoo, J., Ryu, Y.S., 2007. Controlled drug release using nanoporous anodic aluminum oxide on stent. Thin Solid Films 515, 5184–5187.

Khan, W., Farah, S., Nyska, A., Domb, A.J., 2013. Carrier free rapamycin loaded drug eluting stent: in vitro and in vivo evaluation. J. Controlled Release 168, 70–76.

Kotani, J., Awata, M., Nanto, S., Uematsu, M., Oshima, F., Minamiguchi, H., Mintz, G.S., Nagata, S., 2006. Incomplete neointimal coverage of rapamycin-eluting stents. Angioscopic findings. J. Am. Coll. Cardiol. 47 (10), 2108–2111.

Levich, V.G., 1962. Physicochemical Hydrodynamics, second ed. Prentice-Hall, Upper Saddle River, NJ.

Mangina, D., Garciab, E., Gerardc, S., Hoffd, C., Kleina, J.P., Veeslerc, S., 2006. Modeling of the dissolution of a pharmaceutical compound. J. Cryst. Growth 286, 121–125.

Martin, D.M., Boyle, F.J., 2011. Drug-eluting stents for coronary artery disease: a review. Med. Eng. Phys. 33 (2), 148–163.

Marx, S.O., Totary-Jain, H., Marks, A.R., 2011. Vascular smooth muscle cell proliferation in restenosis. Circ. Cardiovasc. Interv. 4, 104–111.

McFadden, E.P., Stabile, E., Regar, E., Cheneau, E., Ong, A.T.L., Kinnaird, T., Suddath, W.O., Weissman, N.J., Torguson, R., Kent, K.M., Pichard, A.D., Satler, L.F., Waksman, R., Serruys, P.W., 2004. Late thrombosis in drug-eluting coronary stents after discontinuation of antiplatelet therapy. Lancet 364, 1519–1521.

McGinty, S., Vo, T.T.N., Meere, M.G., McKee, S., McCormick, C., 2015. Some design considerations for polymer-free drug-eluting stents: a mathematical approach. Acta Biomater. 18, 213–225.

McGinty, S., 2014. A decade of modelling drug release from arterial stents. Math. Biosci. 257, 80–90.

Mehran, R., Dangas, G., Abizaid, A.S., Mintz, G.S., Lansky, A.J., Satler, L.F., Pichard, A.D., Kent, K.M., Stone, G.W., Leon, M.B., 1999. Angiographic patterns of in-stent restenosis: classification and implications for long-term outcome. Circulation 100, 1872–1878.

Mohr, F.W., Morice, M.C., Kappetein, A.P., Feldman, T.E., Stahle, E., Colombo, A., Mack, M.J., Holmes, D.R., Morel, M.A., Van Dyck, N., Houle, V.M., Dawkins, K.D., Serruys, P.W., 2013. Coronary artery bypass graft surgery versus percutaneous coronary intervention in patients with three-vessel disease and left main coronary disease: 5-year

follow-up of the randomised, clinical syntax trial. Lancet 381, 629–638.

O'Brien, C.C., Kolachalama, V.B., Barber, T.J., Simmons, A., Edelman, E.R., 2013. Impact of flow pulsatility on arterial drug distribution in stent-based therapy. J. Controlled Release 168, 115–124.

Pache, J., Dibra, A., Mehilli, J., Dirschinger, J., Schomig, A., Kastrati, A., 2005. Drug-eluting stents compared with thin-strut bare stents for the reduction of restenosis: a prospective, randomized trial. Eur. Heart J. 26, 1262–1268.

Park, S.J., Ahn, J.M., Kim, Y.H., Park, D.W., Yun, S.C., Lee, J.Y., Kang, S.J., Lee, S.W., Lee, C.W., Park, S.W., Choo, S.J., Chung, C.H., Lee, J.W., Cohen, D.J., Yeung, A.C., Hur, S.H., Seung, K.B., Ahn, T.H., Kwon, H.M., Lim, D.S., Rha, S.W., Jeong, M.H., Lee, B.K., Tresukosol, D., Fu, G.S., Ong, T.K., 2015. Trial of everolimus-eluting stents or bypass surgery for coronary disease. N. Engl. J. Med. 372, 1204–1212.

Peppas, N.A., Narasimhan, B., 2014. Mathematical models in drug delivery: how modeling has shaped the way we design new drug delivery systems. J. Controlled Release 190, 75–81.

Siepmann, J., Siepmann, F., 2008. Mathematical modeling of drug delivery. Int. J. Pharm. 364, 328–343.

Siepmann, J., Siepmann, F., 2013. Mathematical modeling of dissolution. Int. J. Pharm. 453, 12–24.

Stone, G.W., Ellis, S.G., Cannon, L., Mann, J.T., Greenberg, J.D., Spriggs, D., O'Shaughnessy, C.D., DeMaio, S., Hall, P., Popma, J.J., Koglin, J., Russell, M.E., 2005. Comparison of a polymer-based paclitaxel-eluting stent with a bare metal stent in patients with complex coronary artery disease. J. Am. Med. Assoc. 294 (10), 1215–1223.

Topol, E.J., Teirstein, P.S., 2015. Textbook of Interventional Cardiology, seventh ed. Elsevier, Philadelphia.

Translumina Therapeutics, Microporous Surface, http://translumina.in/technology/technology-microporus-surface (accessed: 04.01.16).

Tsujino, I., Ako, J., Honda, Y., Fitzgerald, P.J., 2007. Drug delivery via nano-, micro and macroporous coronary stent surfaces. Expert Opin. Drug Deliv. 4 (3), 287–295.

Tzafriri, A.R., Groothuis, A., Price, G.S., Edelman, E.R., 2012. Stent elution rate determines drug deposition and receptor-mediated effects. J. Controlled Release 161, 918–926.

Tzur-Balter, A., Young, J.M., Bonanno-Young, L.M., Segal, E., 2013. Mathematical modeling of drug release from nanostructured porous Si: combining carrier erosion and hindered drug diffusion for predicting release kinetics. Acta Biomater. 9, 8346–8353.

Virmani, R., Guagliumi, G., Farb, A., Musumeci, G., Grieco, N., Motta, T., Mihalcsik, L., Tespili, M., Valsecchi, O., Kolodgie, F.D., 2004. Localized hypersensitivity and late coronary thrombosis secondary to a rapamycin-eluting stent: should we be cautious? Circulation 109 (6), 701–705.

Wessely, R., Hausleiter, J., Michaelis, C., Jaschke, B., Vogeser, M., Milz, S., Behnisch, B., Schratzenstaller, T., Renke-Gluszko, M., Stöver, M., Wintermantel, E., Kastrati, A., Schömig, A., 2005. Inhibition of neointima formation by a novel drug-eluting stent system that allows for dose-adjustable, multiple, and on-site stent coating. Arterioscler. Thromb. Vasc. Biol. 25, 748–753.

Whitehouse, D.J., 2002. Surfaces and their Measurement. first ed. Hermes Penton Ltd, London.

The World Health Organisation, Fact Sheet No. 310, Updated May 2014, http://www.who.int/mediacentre/factsheets/fs310_2008.pdf (accessed: 05.05.16).

Yinyi Biotech, http://www.dlyinyi.com/yaowu-en.php (accessed: 15.12.16).